On the Ionization State of the Substrate in the Active Site of Glutamate Racemase. A QM/MM Study about the Importance of Being Zwitterionic†

Eduard Puig,‡ Mireia Garcia-Viloca,*,§ Àngels González-Lafont,‡,§ and José M. Lluch‡,§

Departament de Química, Universitat Autònoma de Barcelona, Bellaterra (Barcelona), Spain, and Institut de Biotecnologia i de Biomedicina, Universitat Autònoma de Barcelona, Bellaterra (Barcelona), Spain

Received: August 13, 2005; In Final Form: November 7, 2005

Computer simulations on a QM/MM potential energy surface have been carried out to gain insights into the catalytic mechanism of glutamate racemase (MurI). Understanding such a mechanism is a challenging task from the chemical point of view because it involves the deprotonation of a low acidic proton by a relatively weak base to give a carbanionic intermediate. First, we have examined the dependency of the kinetics and thermodynamics of the racemization process catalyzed by MurI on the ionization state of the substrate (glutamate) main chain. Second, we have employed an energy decomposition procedure to study the medium effect on the enzyme−substrate electrostatic and polarization interactions along the reaction. Importantly, the present theoretical results quantitatively support the mechanistic proposal by Rios et al. [*J. Am. Chem. Soc.* **2000**, *122*, 9373−9385] for the PLP-independent amino acid racemases.

1. Introduction

The natural amino acids present in proteins are of the L-form and show a high degree of stereochemical integrity. The α-carbon (Cα), the estereogenic center, cannot easily invert its configuration because of the low acidity of the α-proton (Hα). Some enzymes though, are able to change the stereochemistry of the amino acids by first breaking the stable Cα−Hα bond and then obtaining the corresponding enantiomer of the D-form.[1−3]

D-Amino acids can be found in vertebrates including humans. But they are best well-known as an essential components of peptidoglycan, the rigidyfing component of the bacterial cell wall that protects the organism from osmotic lysis.[4] D-Amino acids do not need to be synthesized and are obtained from the more abundant L-amino acids thanks to the racemase enzymes function. Glutamate racemase (MurI) is one of these enzymes. It provides bacteria with a source of D-glutamate by catalyzing the interconversion of the glutamate enantiomers. D-Glutamate is one of the components of peptidoglycan, and for this reason the inhibition of MurI is an attractive target for the design of antibacterial agents.[5]

The glutamate racemase mechanism involves the deprotonation of the substrate at the Cα position by an anionic cysteine residue, forming a carbanionic intermediate, followed by a reprotonation in the opposite stereochemical sense by another cysteine[6−8] (see Figure 1). Though most of the amino acid racemases use the cofactor pyridoxal phosphate (PLP), MurI does not use any cofactor nor metal ion to achieve the difficult abstraction of the Hα and it is then classified as a PLP-independent amino acid racemase, together with the enzymes aspartate racemase[9] and proline racemase.[10−12] Understanding the reaction mechanism of MurI is a challenging task from the chemical point of view because it involves the deprotonation of a low acidic proton by a relatively weak base.

One of the main functions of the enzyme should be to acidify as much as posible the Hα of the substrate. The acidity of this proton is highly dependent upon the ionization state of the main chain of the amino acid. As shown in Figure 2, there are three possible ionization states for the amino acids main chain, which we have named as anionic, zwitterionic, or cationic, on the basis of the main chain charge. In any proposal about the racemase catalytic mechanism we should consider the differential con-

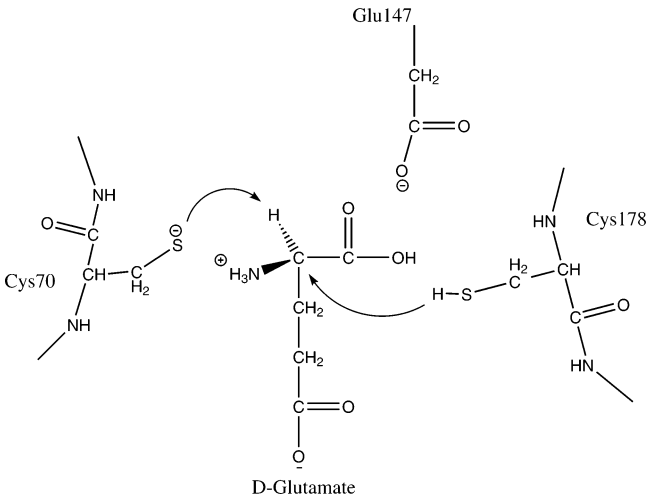

Figure 1. Schematic representation of the enzymatic α-proton abstraction/reprotonation mechanism in the active center of MurI.

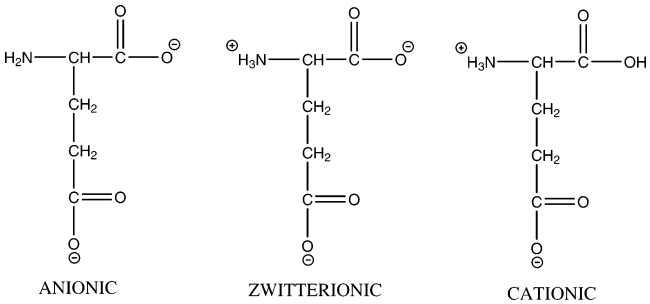

Figure 2. Schematic representation of the three possible ionization states of glutamate main chain.

† Part of the special issue "Donald G. Truhlar Festschrift".
‡ Departament de Química.
§ Institut de Biotecnologia i de Biomedicina.

10.1021/jp054555y CCC: $33.50
Published on Web 11/25/2005

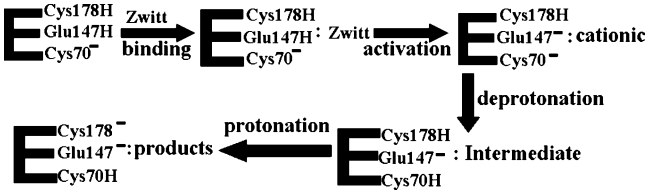

Figure 3. Schematic representation of the catalytic mechanism proposed by Rios et al.[16] for the PLP-independent amino acid racemases.

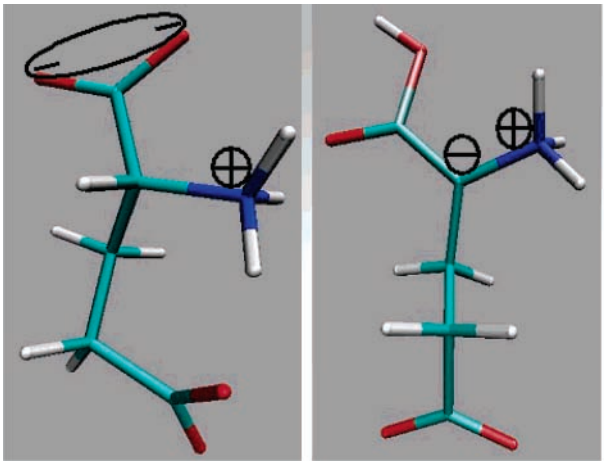

Figure 4. Comparison of the main chain charges in the zwitterion (left) and in the intermediate (right).

centration and reactivity of the three species in the enzyme active site. At the pH optimum of *A. pyrophilus* MurI(pH 8.5),[13] the most abundant ionization state is the zwitterionic main chain. Moreover, deprotonation from the Cα of either the zwitterionic or the cationic main chain species to yield an ylide will be favored compared to the formation of the carbanion from deprotonation of the anionic main chain species.[14] Of these two favored processes, the deprotonation from the cationic main chain is further activated by the lower pK_a of the Hα proton in this state; however, to achieve this ionization state, a low pH environment is needed, which is not suitable for the reaction because the catalytic basis (cysteines) will be protonated. Nevertheless, Rios et al.[15,16] have proposed a general mechanism for the PLP-independent amino acid racemase enzymes that proceeds through the cationic main chain ionization state (see Figure 3). According to this mechanism, the enzyme binds the more abundant substrate species with a zwitterionic main chain. Then the enzyme activates the bound zwitterion toward the formation of the ylide intermediate by a proton transfer (from our simulations the proton would come from the residue Glu147) to the main chain carboxylate, and then the deprotonation/protonation mechanism by the catalytic thiolate/thiol cysteines would lead to the enantiomeric conversion. Moreover, they argue that in comparison to water, the enzyme binds the ylide intermediate, generated after the Hα deprotonation, more tightly than the substrate amino acid zwitterion, because the more desolvated active site of the enzyme enhances the intramolecular interaction between the more closely spaced opposite charges in the former species. In Figure 4 the location of the opposite charges in the two species can be compared. This proposal is supported by the crystallographic analysis of MurI which shows that the substrate analogue glutamine is bound at a deep pocket sequestered from the solvent.[17]

Thus, Rios et al.[16] propose two main roles of the PLP-independent racemases: (1) to activate the bound zwitterion toward enolization via the proton transfer from an enzymatic residue to the carboxylate group of the main chain of the substrate and (2) to enhance the intermediate intramolecular stabilization by providing a less shielded environment in comparison to water. In this work, we will quantitatively examine both proposals in the case of MurI enzyme by carrying out computer simulations on a model of the enzyme−substrate complex that has been obtained from a previous study of the binding of the ligand in the enzyme active site.[18] The results of that study indicate that there exist at least three different modes of binding of the substrate with a zwitterionic main chain in the active site of MurI. From the three main modes of binding, we have been able to estimate the most suitable for reaction.

In this paper we will first examine the reactivity of the substrate with a zwitterionic or a cationic main chain, by taking as starting structures (a) the previously obtained model of the substrate−enzyme complex[18] and (b) a second structure that has been built from the first one by transferring the proton of the enzymatic residue Glu147, which was modeled as protonated in our previous study, to the substrate main chain carboxylate group (see Figure 1). It is worthy to note that the hydrogen bond interaction between Glu147, which has been proposed to play an important role in binding and/or catalysis,[17] and the substrate is maintained along our previous molecular dynamics simulation.[18] From these two starting structures, we have simulated the racemization reaction on a hybrid potential energy surface. As a third possibility, we did preliminary simulations on a third model to examine the reactivity of the substrate with an anionic main chain, but we were not able to reproduce the racemization process. These initial unsuccessful results, together with the experimental background provided by the works of Richard[14−16,19,20] and Tanner,[6−8,21−23] discouraged us to further study this model. In contrast, the results of Möbitz and Bruice[24] suggest that this might be a reactive state of the substrate.

Second, we will address the proposal of the preferred binding of the intermediate ylide by the enzyme in comparison to water by means of an energy decomposition procedure that was originally developed for the study of small organic compounds in solution[25] and has been used recently to study electrostatic interactions between a substrate or an inhibitor in an enzyme active site.[26,27]

2. Methods and Simulation Details

2.1. Initial Setup. *2.1.1. Models of the Enzyme−Ligand Complex.* In a previous work[18] we performed several classical molecular dynamics simulations to test different modes of binding of the substrate D-glutamate in its zwitterionic ionization state in the enzymatic active site. We showed there that the model that we called D-Glu-modeled would be a good starting point to begin a reactivity study.

From the previous 1.2 ns classical molecular dynamics simulation of the D-Glu-modeled model, we calculated in this paper the average position of the heavy atoms of the ligand and the protein. The system was reprotonated using the HBUILD facility in the program CHARMM.[28] Then, it was minimized using the ABNR algorithm[28] for 20 steps to relieve bad contacts. The final protein structure was solvated with a previously equilibrated box of water molecules, centered at the geometric center of the protein−substrate complex. The initial dimensions of the box were 100.24 × 69.55 × 62.78 Å^3. Water molecules that were within 2.2 Å of any non-hydrogen atom of the protein or ligand were removed. The resulting system had a net charge of +14, which was neutralized by replacing those waters standing in high potential energy zones and 20 Å away from the active site by chlorides. Subsequently, the anions and waters (the solvent) were minimized for 100 steps, followed by a

restrained minimization of all the system, where a harmonic force of 10 kcal/(mol Å^2) was applied to the backbone atoms of the protein.

To equilibrate the solvated protein system, we first carried out molecular dynamics simulations using the all-atom CHARMM22 force field[29] to represent the protein and the substrate, and using the three-point-charge TIP3[30] model for water. The system was heated gradually without restraints from 0 to 300 K in 30 ps; then it was equilibrated for 70 ps using classical molecular dynamics in the isothermal−isobaric ensemble (NPT) at 1 atm. These calculations were carried out using periodic boundary conditions with the CRYSTAL module of CHARMM version c29, which allows us to reduce the computational burden by only generating the images of those atoms in a given cutoff. In the present study a cutoff of 11.5 Å was used for the nonbonded interactions along with a switch function in the region from 10.5 to 11.5 Å to smoothly reduce the interaction energy to zero. The nonbonded pair list and the image list were built on the basis of group separations, and were updated every 30 and 120 steps, respectively. The relative dielectric constant was set to 1. The equations of motion were propagated using the Leap-Frog integrator with a time step of 1 fs and with the extended system constant pressure and temperature algorithm implemented in CHARMM. All bond lengths involving hydrogen atoms were constrained by the SHAKE algorithm.[31]

The last configuration after the equilibration of the system at 300 K has been used as the starting configuration of the Michaelis complex to initiate the exploration of the PES. To reduce the computational cost, the water box was replaced by a previously equilibrated water sphere of 24 Å radius centered at the Cα. The system was then minimized with a gradient tolerance of 0.001 kcal/(mol Å) without any cutoff for the nonbonded interactions. From the resulting configuration we built the PES for the racemization of the substrate D-glutamate with a zwitterionic main chain.

The initial configuration to calculate the PES for the racemization of the substrate D-glutamate with a cationic main chain was the result of transferring the proton of the Glu147 residue to the main chain carboxylate of the glutamate ligand in the previous minimized structure.

2.1.2. Potential Energy Function. To examine the reactivity of the substrate with a zwitterionic or a cationic main chain, a QM/MM method[32−34] is needed to describe the bonds that should break and the bonds that should be formed for the stereochemical change to take place. In the present study the QM region has a total of 58 atoms, including the glutamate ligand, the two catalytic cysteine side chains, and other residue moieties that are expected to significantly influence the reaction: Asp7, Glu147, and His180. The AM1 semiempirical method[35] was employed as the QM potential.

The MM part of the system and the classical QM/MM electrostatic interactions are described by the CHARMM22 force field. The QM/MM frontier has been treated with the generalized hybrid orbital (GHO) method.[36] The five GHO atoms were Cys70, Cys178, Asp7, and His180 α-carbons, and the Glu147 β-carbon.

The QM/MM van der Waals interactions were recalibrated. The CHARMM22 van der Waals parameters are expected to work between MM atoms belonging to this force field, but they may not describe correctly a MM-QM(AM1) interaction. The new parameters were obtained following the procedure described by Freindorf and Gao[37] and applied recently by Ferrer et al.[38]

2.1.3. Reaction Coordinates and Optimization Details. Reduced potential energy surfaces for the racemization of both the zwitterionic main chain and the cationic main chain glutamate have been generated to study the dependence of the energetics of the enantiomeric interconversion on the ionization state of the glutamate substrate.

As the chemical reaction is composed of two elementary proton transfers, the process can be described by a two-dimensional (2D) potential energy surface. The two coordinates used in this study to define the 2D-PESs are the antisymmetric combination of the distances involving the Hα deprotonation from the Cα by the Cys70 sulfur,

$$\mathrm{RC1} = r_{\mathrm{C\alpha-H\alpha}} - r_{\mathrm{H\alpha-C70S}} \quad (1)$$

and the antisymmetric combination of distances involving the protonation of the Cα by the Cys178 SHγ.

$$\mathrm{RC2} = r_{\mathrm{C178S-H\gamma}} - r_{\mathrm{H\gamma-C\alpha}} \quad (2)$$

We have also used a one-dimensional (1D) reaction coordinate that takes into account both processes (deprotonation and protonation) at the same time to calculate 1D potentials energy profiles.

$$\mathrm{RC4} = \mathrm{RC1} + \mathrm{RC2} \quad (3)$$

The 2D-PESs and 1D-potentials have been obtained by a series of geometry optimizations of the mobile part of the system (see below) in the presence of harmonic restraints applied on the reaction coordinates (RC1 and RC2 or RC4, for the 2D-PESs and 1D-profiles, respectively) used to drive the racemization process. The RESD module in CHARMM was used to define harmonic restraint terms of the form

$$V_{\mathrm{RESD}} = \frac{1}{2}k_{\mathrm{RESD}}(\mathrm{RC} - \mathrm{RC}_{\mathrm{REF}})^2 \quad (4)$$

where k_{RESD} is the restraining force constant, which was set equal to 2500.0 kcal/(mol Å^2). The quantity $\mathrm{RC}_{\mathrm{REF}}$ is the reference value of the reaction coordinate RC at each energy minimization calculation. A step size of 0.1 Å was used during the 2D and 1D scans. For each of the points defined by ($\mathrm{RC1}_{\mathrm{REF}}$, $\mathrm{RC2}_{\mathrm{REF}}$) or $\mathrm{RC4}_{\mathrm{REF}}$, a minimization was carried out with a gradient tolerance of 0.001 kcal/(mol Å) and with the ABNR algorithm. In these restrained minimizations the reaction coordinate was projected out of the gradient. All the atoms 24 Å away from the Cα of the substrate glutamate were kept frozen during the optimizations; that is, 7285 atoms were allowed to move out of 10814. For the nonbonded interactions, a cutoff of 13 Å was used with a switching function from 12 to 13 Å. The nonbonded list was updated every 100 steps.

In addition, the conjugate peak refinement (CPR) algorithm[39] was used to find a smooth reaction path and to localize intermediates and saddle points along that path. Selected structures of the 1D-potentials and 2D-PESs were used as input for the CPR algorithm. The mobile part of the system, the cutoffs, and the optimization criterion used in the CPR calculations were the same as in the RESD minimizations.

2.2. Electrostatic Interaction Energy between the Substrate D-Glutamate and the Environment. *2.2.1. Energy Decomposition Method.* In the present work, we have calculated the total electrostatic interaction energy between the ligand and two different media: the enzyme−water and the aqueous solution, for two states of the ligand along the enzymatic

mechanism proposed by Rios et al.[16] Following the methodology developed by Gao and Xia,[37] we have treated the ligand quantum mechanically by the semiempirical AM1 method[35] and the surrounding media (protein amino acids or/and solvent) has been represented classically with the CHARMM22[29] or the TIP3P[30] model, respectively. The electrostatic interaction energy between the ligand (QM) and the environment (MM) is

$$\Delta E_{el} = \langle \Psi | \hat{H}^0_{QM} + \hat{H}_{QM/MM} | \Psi \rangle - \langle \Psi^0 | \hat{H}^0_{QM} | \Psi^0 \rangle = E_{QM} + E_{QM/MM} - E^0_{QM} \quad (5)$$

where Ψ and Ψ^0 refer to the wave functions of the ligand in the protein environment and in the gas phase, respectively. ΔE_{el} can be decomposed into a permanent interaction energy (ΔE_{perm}), corresponding to the interaction energy between an unpolarized substrate molecule with the environment and a polarization energy (ΔE_{pol}) as a result of the change in the molecular wave function in the enzyme or aqueous solution. Thus, the total electrostatic interaction energy between the substrate and the environment is written as

$$\Delta E_{el} = \Delta E_{perm} + \Delta E_{pol} \quad (6)$$

In eq 6, the permanent interaction energy is computed using the wave function of the substrate in the gas phase through the QM/MM electrostatic interaction Hamiltonian:

$$\Delta E_{perm} = \langle \Psi^0 | \hat{H}_{QM/MM} | \Psi^0 \rangle \quad (7)$$

The polarization energy can be further decomposed into a polarization stabilization term (the increase in interaction energy of the substrate due to its new charge distribution in condensed phase) and a substrate electronic distortion term (energetic penalty for reorganizing the electron distribution):

$$\Delta E_{pol} = \Delta E_{stab} + \Delta E_{dist} \quad (8)$$

We have computed ΔE_{el} and its components for the four systems: zwitterion reactant complex in water, intermediate ylide in water, zwitterion reactant complex in the enzyme, and intermediate ylide in the enzyme.

2.2.2. Setup and Computational Details. To model the zwitterion reactant complex in water, we solvated glutamate with a cubic box of 37.4027 × 37.4027 × 37.4027 Å^3 of previously equilibrated waters. Those waters with their oxygen atoms closer than 2.2 Å to the ligand were deleted. The solvent was then minimized for 80 steps with the ABNR algorithm. Classical molecular dynamics simulations were carried out with periodic boundary conditions using the CRYSTAL module of CHARMM. The system was heated until 358 K in 30 ps, and then it was equilibrated for 100 ps using a time step of 2 fs with the Leap-Frog integrator in the NPT ensemble. Next, the ligand was described with the AM1 potential and the water molecules with the TIP3P model. The system was minimized for 100 steps with the ABNR method to adapt the ligand to the new potential. The average length of the box edge in the last 10 ps of the previous classical MD simulation was 37.6 Å, and it was used in the next QM/MM dynamics simulations in the NVT ensemble at 358 K for 125 ps. We collected the average ΔE_{el} of the ligand from the last 25 ps. To model the intermediate ylide in water, the Hα proton was transferred from the Cα to the main chain carboxylate. The same cubic box of 37.6 Å edge was used to solvate the intermediate ylide. MD simulations in the NVT ensemble were carried out at 358 K for 125 ps, collecting the average ΔE_{el} of the ligand from the last 25 ps.

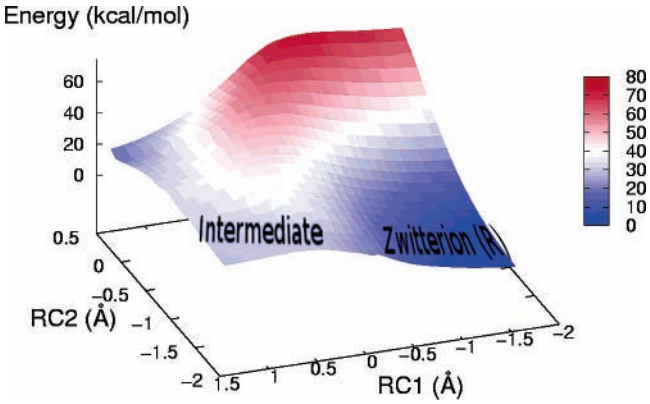

Figure 5. Potential energy surface at the AM1/MM level for the racemization of the D-glutamate substrate with a zwitterionic main chain. RC1 and RC2 are the coordinates associated to the deprotonation and reprotonation processes (see eq 1 and eq 2).

The zwitterion reactant complex in the enzyme was modeled from the already equilibrated structure at 300 K using periodic boundary conditions in the NPT ensemble (see section 2.1.1). Then, the ligand was defined as the QM(AM1) part of the system and the rest of the enzyme and solvent as the MM part. The system was minimized for 80 steps to adapt it to the new potential. Next, we carried out QM/MM molecular dynamics simulations in the NVT ensemble. The dimensions of the orthogonal water box were fixed at 100.2 × 69.6 × 62.8 Å^3, which were the average edge lengths of the last 70 ps. The system was heated until 358 K in 10 ps. Then it was equilibrated for 125 ps of MD simulations. The average ΔE_{el} of the ligand was taken from the last 25 ps. The intermediate ylide in the enzyme was modeled starting from the equilibrated structure of the reactant complex at 300 K too. The Hα proton was removed, the main chain carboxylate and the Cys70 were protonated and the Glu147 was deprotonated. The intermediate was defined as the QM subsystem and the rest as the MM part. Then, the whole system was minimized for 80 steps. We solvated the system with the same orthogonal water box used for the zwitterion reactant complex. QM/MM molecular dynamics simulations in the NVT ensemble. The system was heated until 358 K in 10 ps of MD simulations in the NVT ensemble. Then it was equilibrated for 125 ps, and the average ΔE_{el} of the ligand was taken from the last 25 ps.

3. Results and Discussion

3.1. Energy Profiles. *3.1.1 Reactivity of the* D*-Glutamate Substrate with a Zwitterionic Main Chain Group.* Figure 5 shows the 2D-PES obtained when exploring the racemization of the substrate D-glutamate with a zwitterionic main chain. At the bottom right corner of the figure we can locate a reactant zone corresponding to negative values of RC1 (−1.5 Å) and RC2 (−2.0 Å). The optimized structures of this region correspond to the reactant configuration with the thiolate group of Cys70 pointing the Hα of D-glutamate with an interaction distance of ∼4 Å. The 2D PES exploration also leads to an intermediate zone along a stepwise mechanism (RC1 1.5 Å and RC2 1.8 Å), where we found that the optimized structures resemble the carbanionic planar intermediate formed after the deprotonation of the substrate by Cys70. However, the progress of that pathway to the structures found at positive values of RC1 and RC2 (top left corner of Figure 5) does not lead to the racemization product but tends to revert to the reactant.

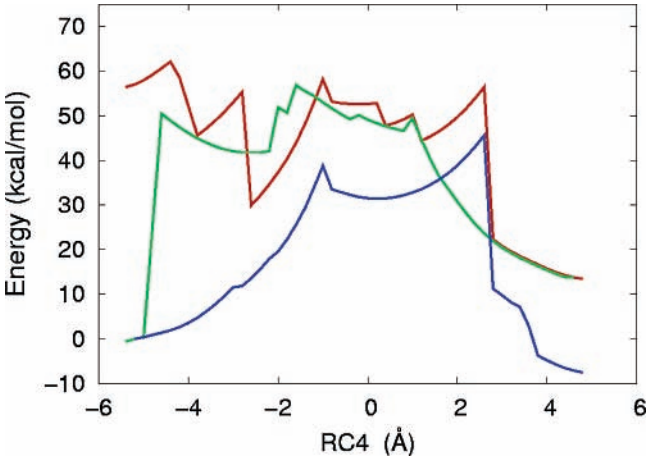

Figure 6. RESDs paths of the zwitterionic main chain carboxylate as a function of the RC4 coordinate (see eq 3); path1 from D-Glu to L-Glu (red); path2 from L-Glu to D-Glu (green); path3 from D-Glu to L-Glu (blue).

TABLE 1: Relevant Geometrical Changes and Relative Energy (D-Glu in Paths 1 and 3 and L-Glu in Path2) during the Enantiomeric Conversion Corresponding to the RESD Paths[a]

	$r_{H\alpha-C70S}$	$r_{C\alpha-H\alpha}$	$r_{H\gamma-C\alpha}$	$r_{C178S-H\gamma}$	dihed(N,Cα,Cβ,O)	energy
Path1: D-Glu ⟹ L-Glu						
reactants	4.29	1.14	3.59	1.35	126.91	0.00
TS1	1.64	1.46	2.31	1.48	138.40	1.73
Inter	1.35	3.92	2.94	1.36	173.21	−6.19
TS2	1.34	4.80	2.29	1.43	154.62	0.02
products	1.35	3.82	1.14	3.26	124.36	−42.97
Path2: D-Glu ⟸ L-Glu						
reactants	1.35	3.82	1.14	3.27	124.44	0.00
TS1	1.45	2.34	1.49	1.61	141.54	35.71
Inter	1.38	3.33	5.68	1.33	178.09	28.02
TS2	1.44	2.41	6.89	1.32	149.53	36.69
products	4.12	1.14	3.56	1.34	126.52	−14.35
Path3: D-Glu ⟹ L-Glu						
reactants	4.31	1.14	3.58	1.35	127.83	0.00
TS1	1.60	1.49	2.35	1.46	139.60	38.77
Inter	1.36	3.60	3.17	1.33	175.87	31.47
TS2	1.34	4.81	2.30	1.43	155.59	45.57
products	1.35	3.81	1.14	3.28	124.49	−7.12

[a] Distances are in Å, dihedral angles in degrees, and energies in kcal/mol.

From this negative result we have concluded that the minimization procedure used to define a reduced 2D-PES is not adequate to follow the MurI reaction mechanism with a zwitterion substrate bound in the active center of the enzyme.

In contrast, the restrained minimizations at different points of the more flexible reaction coordinate RC4 (see eq 3) succeed to localize a minimum energy path for the racemization of the zwitterionic D-glutamate in the active site of MurI. In fact, we have calculated three different paths by driving the reaction coordinate from reactants to products and repeating back and forward the 1D-PES exploration. As shown in Figure 6, the obtained potential energy profiles, which we have named RESD path1, RESD path2, and RESD path3, do not converge. This is a well-known problem due to the use of a too simple reaction coordinate to study the reaction mechanism of a complex system. Table 1 gives the most relevant bond distances and the relative energies of the maxima and minima located along the three RESD paths. We think that the energetic differences between the potential energy profiles is mainly due to conformational changes of the degrees of freedom that are not directly involved in the reaction. To confirm this hypothesis, we have

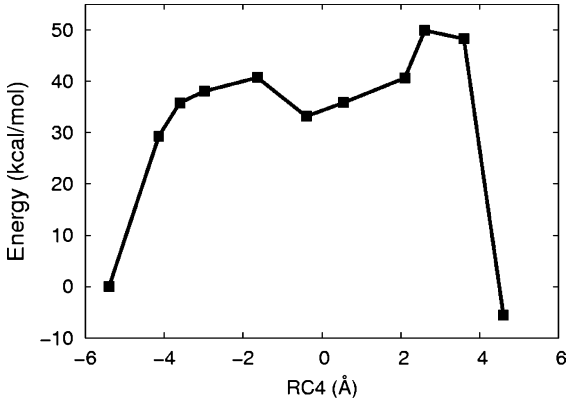

Figure 7. Conjugate peak refinement path for the zwitterionic main chain glutamate.

TABLE 2: Relevant Geometrical Changes and Relative Energy during the Enantiomeric Conversion (D-Glu ⟹ L-Glu) Corresponding to the CPR Path for the Zwitterionic Main Chain Glutamate[a]

	zwitterionic					
CPR	$r_{H\alpha-C70S}$	$r_{C\alpha-H\alpha}$	$r_{H\gamma-C\alpha}$	$r_{C178S-H\gamma}$	dihed(N,Cα,Cβ,O)	energy
reactants	4.31	1.14	3.57	1.35	127.81	0.00
TS1	1.49	1.88	3.37	1.33	137.45	40.73
Inter	1.36	2.90	3.26	1.32	164.59	33.17
TS2	1.37	4.24	1.83	1.56	142.16	49.90
products	1.35	3.81	1.14	3.28	124.44	−5.60

[a] Distances are in Å, dihedral angles in degrees, and energies are in kcal/mol.

carried out AM1 single point energy calculations on only the QM subsystem, removing all the MM atoms and saturating the GHO atoms with protons at the structures of the RESD paths, which has led to more converged profiles. Then, the conjugated peak refinement algorithm,[39] implemented in the TRAVEL module of CHARMM has been used to obtain a unique path through the potential energy surface without imposing any predeterminate reaction coordinate. The resulting energy profile is shown in Figure 7 in front of the RC4 coordinate. The RESD path3 was used as the input for the CPR algorithm as it presents a smoother energy profile. The CPR was guided through four structures corresponding to the first, the 50th, the 75th and the last of the RESD path3. With less structures the path did not converge.

This method gives a good estimation of the saddle points and intermediates (stationary points) of an enzymatic reaction.[40] Table 2 summarizes the geometrical features and energetics of these approximate stationary points. As shown in Figure 7, the racemization of the substrate D-glutamate with a zwitterionic main chain proceeds via a stepwise mechanism that goes first through the saddle point (40 kcal/mol) of the abstraction of the Hα of the substrate by the catalytic base Cys70, to arrive at a planar intermediate that is reprotonated by Cys178 in a chemical step with a 50 kcal/mol barrier height with respect to reactants. Thus, the two-step mechanism has a global barrier of 50 kcal/mol, which is clearly too high to even be compared to the kinetic data for the MurI reaction.[8] On the other hand, it has to be noted that the main chain carboxylate group of the ylide coming from the zwitterionic reactant has a very high basicity, in such a way that its protonation should occur prior to the reprotonation by the Cys178. Anyway, the reaction coordinate that has been used does not lead us to explore this possibility.

3.1.2. Reactivity of the D*-Glutamate Substrate with a Cationic Main Chain Group.* Figure 8A corresponds to the 2-D PES obtained by using the RC1 and RC2 reaction coordinates to

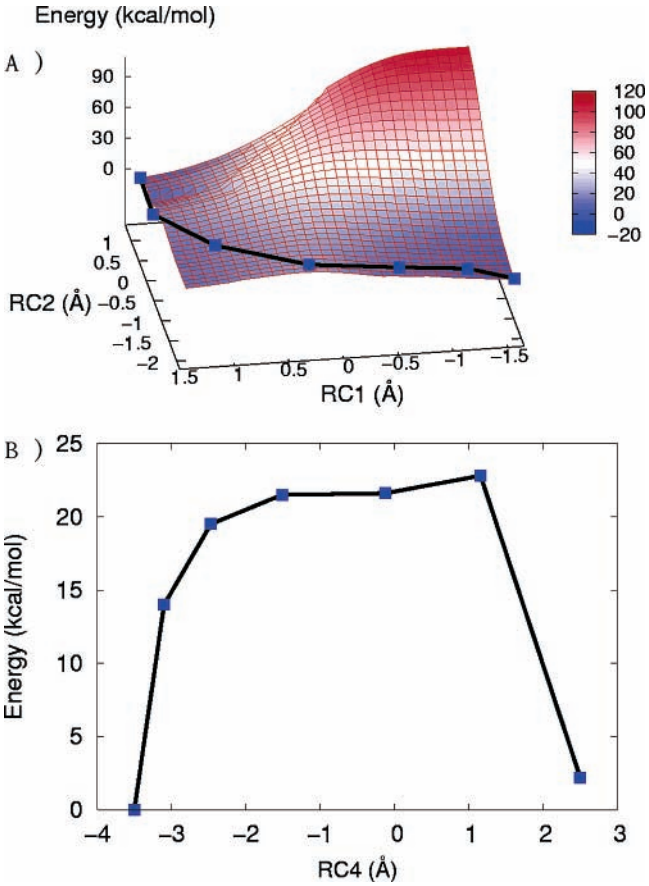

Figure 8. (A) Potential energy surface at the AM1/MM level for the racemization of the D-glutamate substrate with a cationic main chain. RC1 and RC2 are the coordinates associated with the deprotonation and reprotonation processes (see eq 1 and eq 2) and CPR path is superimposed on the PES. (B) CPR path in front of the RC4 coordinate (see eq 3).

drive the racemization of the substrate with a protonated main chain carboxylic group. In contrast to the result found for the zwitterionic ionization state of the substrate, the RESD procedure applied to scan these two coordinates leads to the formation of L-glutamate through a stepwise pathway with a 23 kcal/mol barrier height. As described for Figure 5, on the 2D-PES obtained we can locate three different regions, the reactant region at negative values of the reaction coordinates (RC1 and RC2 ~ -2 Å), the intermediate region at values of RC1 and RC2 close to $+1.5$ and -1.5 Å, respectively, and a product region at the top left corner (RC1 and RC2 ~ 1.5 Å). Importantly, the racemization process has been accelerated by almost 30 kcal/mol by the protonation of the carboxylic main chain group of the substrate. Despite the low QM level used in the present study, which prevents us from giving definitive conclusions, this result quantitatively supports the proposal by Rios et al.[16] that one of the catalytic roles of the PLP-independent racemases is to activate the amino acid substrate toward enolization via a prior proton transfer from the enzyme to the carboxylic main chain of the ligand. In addition, the CPR algorithm has been used to search a smooth minimum energy path on the QM/MM PES, starting from two structures on the 2D-PES, which belong to the reactant, and product region (the first and the last structure generated on the PES). In this case, the CPR path easily converged with only these two structures. The CPR path is shown superimposed on the QM/MM PES in Figure 8A, and as a function of the RC4 coordinate in Figure 8B. The geometrical features and energetics of the approximate stationary

TABLE 3: Relevant Geometrical Changes and Relative Energies during the Enantiomeric Conversion (D-Glu ⟹ L-Glu) along the CPR Path for the Cationic Main Chain Glutamate[a]

	cationic					
CPR	$r_{H\alpha-C70S}$	$r_{C\alpha-H\alpha}$	$r_{H\gamma-C\alpha}$	$r_{C178S-H\gamma}$	dihed(N,Cα,Cβ,O)	energy
reactants	2.77	1.17	3.27	1.37	126.62	0.00
TS1	1.51	1.77	3.13	1.36	143.70	21.50
Inter	1.35	2.38	2.52	1.37	175.93	21.60
TS2	1.34	2.83	1.84	1.51	139.89	22.80
products	1.38	2.78	1.19	2.29	126.32	2.20

[a] Distances are in Å, dihedral angles in degrees, and energies are in kcal/mol.

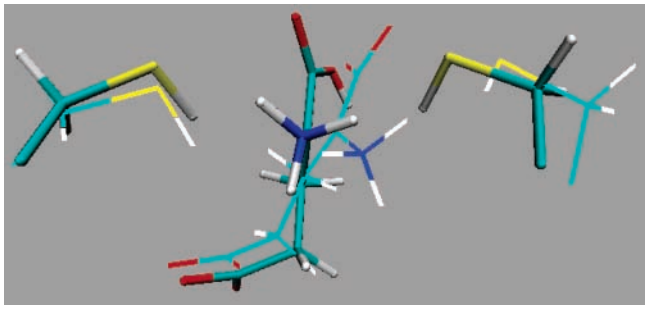

Figure 9. Comparison of the zwitterionic (thick lines) and cationic glutamate intermediates (licorice).

points localized by the CPR algorithm are summarized in Table 3. The comparison between Tables 2 and 3 indicates that the ionization state of the main chain of the substrate determines mainly the energetics but also to a less extent the geometric changes along the racemization process. In fact, in contrast to the CPR profile found for the reactant with zwitterionic main chain, we cannot distinguish in terms of energy between the structures called TS1 and Inter in Table 3. That is, the CPR results suggest that the reaction proceeds through a unique maxima when the reactant has a cationic main chain. However, in this paper, we have not characterized any stationary point, and thus, we cannot predict if there is one, or two saddle points on the very flat intermediate region in Figure 8. Figure 9 compares the geometrical features of the active site at the two different intermediates (structures named Inter in Tables 2 and 3) obtained with the CPR algorithm for the racemization of D-glutamate with the two different (zwitterionic or cationic) main chain ionization states. The analysis of the two structures indicates that the main interactions between the substrate and the active site residues are common for the two intermediates, and this suggest that the lowering of the barrier height for racemization of the cationic substrate comes mainly from the acidification of the Hα upon protonation of the carboxylic main chain group of the substrate.

3.2. Binding of the Intermediate Ylide. *3.2.1. Differential Binding of the Intermediate Ylide by the Enzyme in Comparison to Water.* The two reaction pathways obtained in the previous section, which correspond to the racemization of a zwitterionic or cationic D-glutamate, proceed to an ylide intermediate. From the chemical point of view, the two localized intermediates only differ in the ionization state of the main chain group. Once we have theoretically assessed the mechanistic proposal of Rios et al.[16] which indicates that the most reactive species is the cationic substrate, we examine here the effect of the medium on the relative stabilization of the resulting ylide intermediate with respect to the zwitterionic reactant complex, which is the most abundant ionization state at neutral pH.

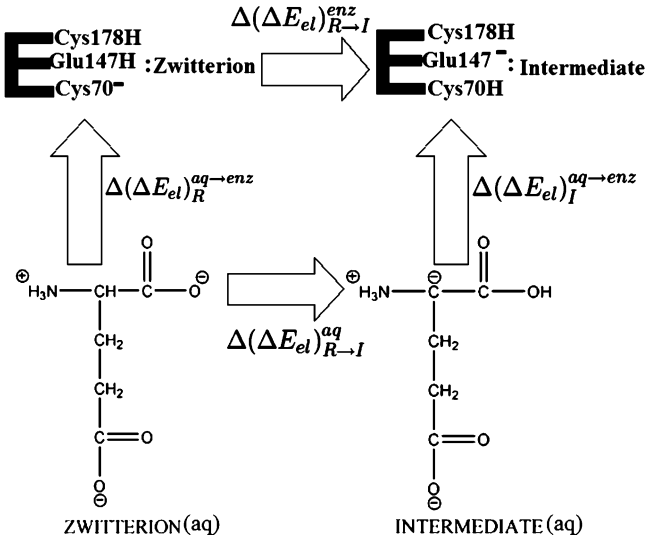

Figure 10. Schematic representation of the thermodynamic cycle for calculating the difference in the electrostatic energy cost of transferring the reactant from water to the active site of MurI relative to the intermediate ylide (see eq 9)

The most standard procedure to theoretically examine the differential binding of the zwitterionic reactant complex and the intermediate ylide in the active site of MurI is to use a free energy simulation technique on a molecular mechanics PES. With these techniques it is possible to quantitatively determine the differential free energy cost of transferring these species from water to the enzyme environment by simulating the enolization reaction in both media. Alternatively, in this work, we have estimated the relative stabilization (in terms of electrostatic interaction energies ligand-environment) of the ylide intermediate in comparison to the zwitterionic reactant complex in each media, as schemed in Figure 10. The result of the calculation gives the difference in the electrostatic energy cost of transferring the reactant from water to the active site of MurI in comparison to the intermediate.

$$\Delta(\Delta E_{el})_R^{aq\rightarrow enz} - \Delta(\Delta E_{el})_I^{aq\rightarrow enz} = \Delta(\Delta E_{el})_{R\rightarrow I}^{aq} - \Delta(\Delta E_{el})_{R\rightarrow I}^{enz} \quad (9)$$

Importantly, the method used is based on the QM/MM approach and includes the effect of the electronic polarization of the ligand by the protein-aqueous environment. The computational results obtained recently from the application of this method to the study of ligand−protein interactions show that explicit treatment of the polarization effect on the ligand is important.[26,27]

Figure 11 indicates that in comparison to the reactant, the ylide intermediate is more stabilized by the enzymatic environment than by the aqueous solution, which qualitatively indicates which one is more tightly bound by the enzyme. In terms of electrostatic energy, the cost of transferring the ylide intermediate from water to the enzyme is 32 kcal/mol less than transferring the reactant zwitterion. However, we cannot give a quantitative result for the binding (free energy cost of transferring the ligand from water into the active site) because the thermal and entropic effects are missing in our calculation.

The analysis of the different energy terms shown in Table 4 can help us to understand the reasons for the preferred binding of the ylide intermediate versus the reactant.

As shown in the first column of Table 4, the zwitterionic reactant is the most stabilized species in both media; however, the difference in the total electrostatic interaction energy between the reactant and the intermediate ylide is highly reduced in the

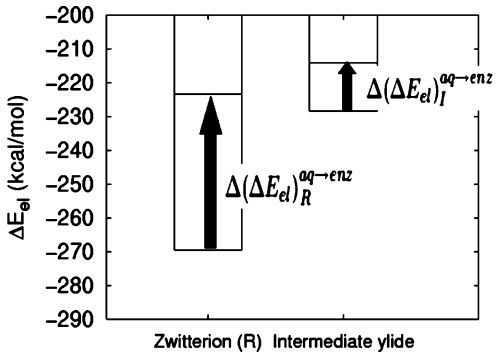

Figure 11. Average results of $\Delta(\Delta E_{el})_R^{aq\rightarrow enz}$ and $\Delta(\Delta E_{el})_I^{aq\rightarrow enz}$ from the Zwitterion and the Intermediate ylide QM/MM dynamics (see eq 9).

TABLE 4: Comparison of the Electrostatic Interaction Energies (kcal/mol) and Their Components for the Zwitterionic Reactant Complex and the Intermediate Ylide Both in Water and in the Enzyme

water	ΔE_{el}	ΔE_{perm}	ΔE_{pol}	ΔE_{stab}	ΔE_{dist}
zwitterion reactant	−270	−249	−21 (8%)	−40	20
intermediate ylide	−229	−211	−17 (7%)	−34	17
$\Delta(\Delta E)_{R\rightarrow I}^{aq}$	41	38	4 (10%)	6	−3
enzyme	ΔE_{el}	ΔE_{perm}	ΔE_{pol}	ΔE_{stab}	ΔE_{dist}
zwitterion reactant	−223	−209	−14 (6%)	−27	13
intermediate ylide	−214	−205	−9 (4%)	−19	9
$\Delta(\Delta E)_{R\rightarrow I}^{enz}$	9	4	5 (55%)	8	−4

enzyme environment. That is, the 41 kcal/mol of differential stabilization that favors the reactant in water is diminished to 9 kcal/mol in the enzyme. This result supports the findings of Williams et al.[41] These authors have estimated a ca. 100 kcal/mol difference in the α-NMe_3^+ substituent effect on oxygen deprotonation of glycine in the gas phase and water. They propose that only a small part of the ca. 100 kcal/mol differential stabilization of the intermediate ylide in the gas phase compared with water needs to be recovered during enzyme-catalyzed formation of a zwitterionic enolate (ylide) at a nonpolar active site for this to make a significant contribution to rate acceleration for the enzymatic reaction. For example, they partially or entirely correlate this effect to the ca. 19 kcal/mol stabilization of the transition state for deprotonation of proline by another PLP-independent racemase, proline racemase. In the case of MurI enzyme, the analysis of the second column of Table 4 indicates that the differential stabilization between the reactant and the intermediate is mainly due to the permanent interaction energy term (see eq 7 in the 2.2.1 section), for which the difference between the values corresponding to the two species is reduced from 38 to 5 kcal/mol. In contrast, the polarization term (third column of Table 4) has a nonnegligible but much smaller effect on the differential binding between the two species, and interestingly, it goes in the contrary direction. That is, looking at the values between parenthesis in Table 4 we can see that the aqueous solution polarizes more than the enzyme both the reactant and the intermediate (8%-7% of polarization in water versus 6%-4% in the enzyme), but the intermediate ylide is relatively less polarized (4%) than the reactant zwittterion (6%) in the enzyme, whereas in water they have nearly the same degree of polarization (8−7% for the zwitterion and the intermediate respectively). As a consequence, the polarization term, slightly destabilizes the intermediate respect to the reactant in going from water to the enzyme. From the above results, and having in mind that the main contribution comes from the electrostatic permanent interaction term and that this term only

TABLE 5: Contributions of Individual Amino Acid Residues to the Stabilization/Destabilization of the Intermediate Ylide Relative to the Zwitterionic Reactant Complex (kcal/mol)

stabilizing residues	ΔE_{el}	destabilizing residues	ΔE_{el}
Asn71	−114.092	Leu141	56.094
Cys70	−77.177	Asp7	17.209
Ser8	−22.817	Thr114	9.423
Ala146	−6.014	Ala69	6.626
Gly9	−3.094	Ala116	4.078
Glu147	−2.264	Glu148	3.999
Phe6	−2.173	Ser74	3.884
Val10	−2.129	Thr72	3.330
Leu13	−1.798	Leu145	2.436
Thr117	−1.633	Val68	1.581
Gly11	−1.578	Tyr123	1.542
Val67	−1.206	Ser120	1.471
Thr14	−0.586	Leu176	1.034
Val37	−0.447	Gly113	0.883
Leu150	−0.396	Ala73	0.567
Ile93	−0.350	Ala75	0.538
Val15	−0.341	Tyr76	0.515
Cys139	−0.256	Val92	0.428
Tyr30	−0.194	Gly91	0.359
Gly149	−0.170		
Leu16	−0.073		
Ile47	−0.042		
Lys137	−0.023		

comprehends intermolecular QM/MM interactions (see eq 7), we suggest that the preferred binding of the ylide intermediate is not an intramolecular effect. As proposed by Williams et al.,[41] the larger distance separation and the more external position of the opposite charges in the reactant than in the intermediate favors the former in a high polarization media, but this effect is reduced in the less polar MurI active site, where the small separation between charges in the ylide intermediate is enough to compensate the loss of intermolecular interactions with the environment when these charges are more buried. This effect can be thought of as a desolvation effect, which has been proposed to have a role in enzyme catalysis. Although in the present work we have not calculated energy differences between the reactant complex and the transition state of the enolization reaction, this is an endothermic process and it is reasonable to suggest that the desolvation effect also might contribute to catalyze it. Similar effects have been found in other enzymes.[42,43]

3.2.2. Contributions of Individual Amino Acids to the Electrostatic Interaction Energies Ligand-environment. An amino acid decomposition analysis has been carried out to investigate the differential stabilization of the reactant and the intermediate by the enzymatic residues. The average contributions of each residue were determined from a set of 50 coordinates saved at an interval of 0.5 ps from 25 ps MD simulations following the initial equilibration. Contributions were computed by sequentially annihilating the classical point charges of amino acid residues, starting from the ones closest to the substrate. At each deletion step, the difference in quantum mechanical electrostatic energy before and after the charge annihilation is defined as the interaction energy of this residue, *I*, with the QM system.[44]

$$\Delta E_I = [E_{QM}(I) - E_{QM}(I-1)] + [E_{QM/MM}(I) - E_{QM/MM}(I-1)] \quad (10)$$

Although the specified contributions from individual residues to the overall protein−substrate interaction depend on the order of annihilation, the results do provide a reasonable estimate of the magnitude of the interaction energy and a good indication

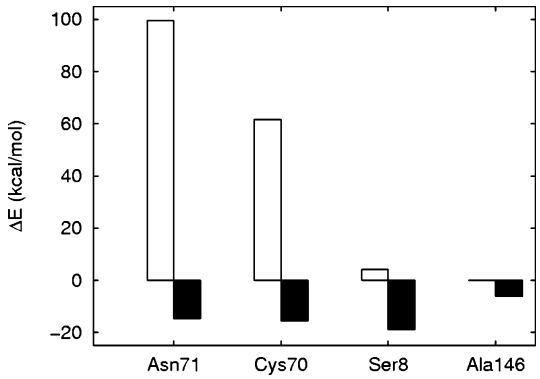

Figure 12. Amino acid residues that contribute more in the stabilization of the intermediate ylide relative to the zwitterionic reactant complex (see Table 5). Electrostatic interaction energy with the zwitterion and the intermediate (positive and negative values, respectively).

of the role of each residue in stabilizing or destabilizing the intermediate ylide.

In Table 5 we show which residues contribute to stabilize or destabilize the intermediate ylide respect to the zwitterionic reactant complex. The table shows that the contribution of the stabilizing residues is much more important than the contribution of the destabilizing ones. In Figure 12 the contribution of the most stabilizing residues have been separated into the interaction with the zwitterionic reactant complex (positive values) and the interaction with the intermediate ylide (negative values). The active site residues Asn71 and Cys70 are by far the most stabilizing residues. As can be seen from the figure, its contribution is mainly due to a destabilizing effect with the zwitterionic reactant complex. The analysis of structures obtained along the MD simulations indicate that the main chain HN proton of the residue Asn71 interacts repulsively with both the Hα proton and the NH_3 group of the ligand. In the intermediate, the interaction with the Hα proton disappears completely because this atom is already attached to Cys70 residue, and the interaction with NH_3 is also weakened as the change in the hybridization of the Cα enlarges the distances between these two groups. Cys70 interacts also negatively with the Hα of the zwitterionic reactant complex. In fact, this destabilizing interaction is the main source of the high energy barrier for the deprotonation reaction to take place from the zwitterionic reactant complex. Other residues such as Ala146 and Ser8 also contribute, but to a minor extent. Unlike Asn71 and Cys70, the contribution of these residues is due to a more stabilizing contribution on the intermediate ylide than a destabilization effect on the zwitterionic reactant complex. On the contrary, residue Ile141 destabilizes the intermediate ylide in comparison to the zwitterionic reactant complex by 56 kcal/mol. This destabilizing effect is difficult to interpret because this residue is far (∼10 Å) from the ligand, and it is clearly compensated by the 114 and 77 kcal/mol stabilizing effect of residues Asn71 and Cys70, respectively.

Thus, apart from the desolvation effect described in the previous section, the active site of MurI also provides a series of individual intermolecular interactions amino acid-substrate that contribute to stabilize the intermediate in comparison to the reactant.

4. Concluding Remarks

The present study highlights important factors in the catalytic mechanism of MurI. Our computational results, in agreement with previous experimental studies[14−16,19,20] suggest at least two possible roles for MurI as a catalyst: (1) to activate the bound

substrate by donating a proton to its carboxylate main chain in a step prior to the racemization process and (2) to optimize the differential stabilization of the intermediate relative to the reactant via an intermolecular effect that comes, partly, from a desolvation effect on the reactant in going from water to the enzyme environment and, partly, from a stabilization effect on the intermediate by the enzymatic residues. Thus, the catalytic effect of glutamate racemase is achieved without resorting to covalent bond formation between the enzyme or cofactor and the transition state.[45]

Acknowledgment. We are grateful for financial support from the Spanish "Ministerio de Ciencia y Tecnologia" and the "Fondo Europeo de Desarrollo Regional" through Project No.BQU2002-00301. M.G.-V. acknowledges the "Ramon y Cajal" program for financial support.

References and Notes

(1) Tanner, M. *Acc. Chem. Res.* **2002**, *35*, 237.
(2) Schnell, B.; Faber, K.; Kroutil, W. *Enzymatic racemisation and its application to synthetic biotransformations* **2003**, *345*, 653.
(3) Yoshimura, T.; Esaki, N. *J. Biosci. Bioeng.* **2003**, *96*, 103.
(4) Doublet, P.; Heijenoort, van J.; Mengin-Lecreulx, D. *Microbial Drug Resistance-Mechanisms Epidemiology and Disease* **1996**, *2*, 43.
(5) Dios, de A.; Prieto, L.; Martin, J. A.; Rubio, A.; Ezquerra, J.; Tebbe, M.; deUralde, B. L.; Martin, J.; Sanchez, A.; LeTourneau, D. L.; McGee, J. E.; Boylan, C.; Parr, T. R.; Smith, M. C. *J. Med. Chem.* **2002**, *45*, 4559.
(6) Gallo, K. A.; Tanner, M. E.; Knowles, J. R. *Biochemistry* **1993**, *32*, 3991.
(7) Glavas, S.; Tanner, M. E. *Biochemistry* **1999**, *38*, 4106.
(8) Glavas, S.; Tanner, M. E. *Biochemistry* **2001**, *40*, 6199.
(9) Liu, L.; Iwata, K.; Kita, A.; Karawasaki, Y.; Yohda, M. *J. Mol. Biol.* **2002**, *319*, 479.
(10) Cardinale, G. J.; Abeles, R. H. *Biochemistry* **1968**, *7*, 3970.
(11) Rudnick, G.; Abeles, R. H. *Biochemistry* **1975**, *14*, 4515.
(12) Albery, W. J.; Knowles, J. R. *Biochemistry* **1986**, *25*, 2572.
(13) Kim, S. S.; Choi, I. G.; Kim, S. H.; Yu, Y. G. *Extremophiles* **1999**, *3*, 175.
(14) Richard, J. P.; Amyes, T. L. *Bioorg. Chem.* **2004**, *32*, 354.
(15) Rios, A.; Richard, J. P. *J. Am. Chem. Soc.* **1997**, *119*, 8375.
(16) Rios, A.; Amyes, T. L.; Richard, J. P. *J. Am. Chem. Soc.* **2000**, *122*, 9373.
(17) Hwang, K. Y.; Cho, C. S.; Kim, S. S.; Sung, H. C.; Yu, Y. G.; Cho, Y. J. *Nature Struct. Biol.* **1999**, *6*, 422.
(18) Puig, E.; Garcia-Viloca, M.; González-Lafont, A.; López, I.; Daura, X.; Lluch, J. M. *J. Chem. Theory Comput.* **2005**, *1*, 737.
(19) Richard, J. P.; Amyes, T. L. *Curr. Opin. Chem. Biol.* **2001**, *5*, 626.
(20) Richard, J. P.; Williams, G.; O'Donoghue, A. C.; Amyes, T. L. *J. Am. Chem. Soc.* **1997**, *119*, S **2002**, *124*, 2957.
(21) Tanner, M. E.; Gallo, K. A.; Knowles, J. R. *Biochemistry* **1993**, *32*, 3998.
(22) Tanner, M. E.; Miao, S. C. *Tetrahedron Lett.* **1994**, *35*, 4073.
(23) Glavas, S.; Tanner, M. E. *Bioorg. Med. Chem. Lett.* **1997**, *7*, 2265.
(24) Mobitz, H.; Bruice, T. C. *Biochemistry* **2004**, *43*, 9685.
(25) Gao, J.; Xia, X. *Science* **1992**, *258*, 631.
(26) Hensen, C.; Hermann, J. C.; Nam, K. H.; Ma, S. H.; Gao, J. L.; Holtje, H. D. *J. Med. Chem.* **2004**, *47*, 6673.
(27) Garcia-Viloca, M.; Truhlar, D. G.; Gao, J. L. *J. Mol. Biol.* **2003**, *327*, 549.
(28) Brooks, B. R.; Bruccoleri, R. E.; Olafson, B. D.; States, D. J.; Swaminathan, S.; Karplus, M. *J. Comput. Chem.* **1983**, *4*, 187.
(29) MacKerell, A. D., Jr.; Bashford, D.; Bellott, M.; Dunbrack, R. L., Jr.; Evanseck, J. D.; Field, M. J.; Fischer, S.; Gao, J.; Guo, H.; Ha, S.; Joseph-McCarthy, D.; Kuchnir, L.; Kuczera, K.; Lau, F. T. K.; Mattos, C.; Michnick, S.; Ngo, T.; Nguyen, D. T.; Prodhom, B.; Roux, B.; Schlenkrich, M.; Smith, J. C.; Stote, R.; Straub, J.; Watanabe, M.; Wiórkiewicz-Kuczera, J.; Yin, D.; Karplus, M. *J. Phys. Chem. B* **1998**, *102*, 3586.
(30) Jorgensen, W. L.; Chandrasekhar, J.; Madura, J.; Impey, R. W.; Klein, M. L. *J. Chem. Phys.* **1983**, *79*, 926.
(31) Ryckaert, J.-P.; Ciccotti, G.; Berendsen, H. J. C. *J. Comput. Phys.* **1977**, *23*, 327.
(32) Warshel, A.; Levitt, M. *J. Mol. Biol.* **1976**, *103*, 227.
(33) Singh, U. C.; Kollman, P. A. *J. Comput. Chem.* **1986**, *7*, 718.
(34) Field, M. J.; Bash, P. A.; Karplus, M. *J. Comput. Chem.* **1990**, *11*, 700.
(35) Dewar, M. J. S.; Zoebisch, E. G.; Healy, E. F.; Stewart, J. J. *J. Am. Chem. Soc.* **1985**, *107*, 3902.
(36) Gao, J.; Amara, P.; Alhambra, C.; Field, M. J. *J. Phys. Chem. A* **1998**, *12*, 4714.
(37) Freindorf, M.; Gao, J. *J. Comput. Chem.* **1996**, *17*, 386.
(38) Ferrer, S.; Ruiz-Pernía, J. J.; Tunón, I.; Moliner, V.; Garcia-Viloca, M.; González-Lafont, A.; Lluch, J. M. *J. Chem. Theory Comput.* **2005**, *1*, 750.
(39) Fischer, S.; Karplus, M. *Chem. Phys. Lett.* **1992**, *194*, 252.
(40) Cui, Q.; Karplus, M. *J. Phys. Chem. B* **2002**, *106*, 1768.
(41) Williams, G.; Maziarz, E. P.; Amyes, T. L.; Wood, T. D.; Richard, J. P. *Biochemistry* **2003**, *42*, 8354.
(42) Devi-Kesavan, L. S.; Gao, J. L. *J. Am. Chem. Soc.* **2003**, *125*, 1532.
(43) A.Shurki,; Strajbl, M.; Villà, J.; Warshel, A. *J. Am. Chem. Soc.* **2002**, *124*, 4097.
(44) Garcia-Viloca, M.; Truhlar, D. G.; Gao, J. L. *Biochemistry* **2003**, *42*, 13558.
(45) Houk, K. N.; Zhang, X. *Acc. Chem. Res.* **2005**, *38*, 379.